PHYSICAL REVIEW B

CONDENSED MATTER AND MATERIALS PHYSICS

THIRD SERIES, VOLUME 57, NUMBER 1 — 1 JANUARY 1998-I

BRIEF REPORTS

Brief Reports are accounts of completed research which, while meeting the usual **Physical Review B** *standards of scientific quality, do not warrant regular articles. A Brief Report may be no longer than four printed pages and must be accompanied by an abstract. The same publication schedule as for regular articles is followed, and page proofs are sent to authors.*

Electron trapping in $PbCl_2$:Tl crystals: The heteronuclear $(PbTl)^{2+}$ center

S. V. Nistor,* E. Goovaerts, and D. Schoemaker

Department of Physics, University of Antwerp (UIA), B-2610 Antwerpen-Wilrijk, Belgium

(Received 19 June 1997)

An EPR study of the Tl^+-doped $PbCl_2$ crystals x-ray irradiated at low temperature reveals the presence, besides known spectra attributed to hole-trapped Tl^{2+} centers and Pb_2^{3+} self-trapped-electron (STEL) centers, of an additional strongly anisotropic set of lines consisting of an intense doublet and several weaker satellite lines spread over a large magnetic-field range. The quantitative analysis of the EPR spectrum shows the corresponding paramagnetic center to be a bent molecular ion $(PbTl)^{2+}$ resulting from electron trapping at a pair of substitutional Pb^{2+} and Tl^+ ions. Its formation suggests the electron trapping at pairs of neighboring cations is a more general characteristic of this material, with possible relevance in photolysis and exciton localization properties. [S0163-1829(98)01002-9]

I. Introduction. Crystalline lead halides PbX_2 (X=Cl, Br, I) are photosensitive materials, i.e., their illumination at room temperature (RT) in the short-wavelength side of the optical absorption (OA) spectrum induces an irreversible photochemical decomposition process with formation of colloidal lead and halogen desorption.[1] The primary defect(s) involved in the photolytic formation of lead colloids has not yet been clearly determined, although it has been suggested that the first step in this process involves the trapping of electrons at lead cations.[1,2] Early electron paramagnetic resonance (EPR) studies on low-temperature UV, x-ray, or γ-ray irradiated $PbCl_2$ single crystals resulted in the identification of some paramagnetic centers with $g \approx 2$ attributed to Pb^+ and Pb_2^{3+} centers,[2–4] an interpretation inconsistent with the more recent results of EPR studies on such centers in alkali and alkali earth halides.[5–9]

Recently we have shown[10,11] that conduction electrons produced by illumination above the band gap in pure $PbCl_2$ crystals are trapped at pairs of nearest-neighbor Pb^{2+} cations along the a axis, resulting in paramagnetic (self-trapped-electron) (STEL) centers. The STEL center represents a paramagnetic Pb_2^{3+} molecular ion with a strongly bent molecular bond and electron configuration complementary to that of the X_2^- (X=halogen) self-trapped hole (STH) center in alkali halides.[12] Its observation strongly supports the proposed new type of self-trapped exciton, in which a hole is trapped in an excited orbital around the heavy electron localized in a state such as the STEL center.[14,15] Moreover, the STEL center may be involved in the formation of lead clusters by photochemical decomposition of lead halides at temperatures where diffusion of anion vacancies occurs.[13]

Here we present the results of an EPR study concerning the electron trapping properties of thallium impurities in $PbCl_2$ crystals, already known[16] to exhibit hole trapping properties. It reports the simultaneous formation, besides the trapped-hole Tl^{2+} centers and STEL centers, of a heteronuclear trapped-electron $(PbTl)^{2+}$ dimer center with bent structure.

II. Experimental. The samples employed in the present study were cut from oxygen-free $PbCl_2$ single crystals doped in the melt with 0.2 mol % of TlCl, prepared by earlier described procedures.[16] After irradiation at T=80 K with x-rays (tungsten cathode, 50 kV, 50 mA) the samples were transferred in the cold region ($T \geqslant 10$ K) of the microwave cavity, without increasing their temperature above 100 K. The EPR measurements were performed with a computer-controlled X-band microwave spectrometer (model ESP-300E, Bruker) equipped with a gas-flow cryogenic system allowing operation in the 10–300 K temperature range.

III. Results. Intense EPR spectra are produced after relatively short (typically 20 min) x-ray irradiation at T=80 K.

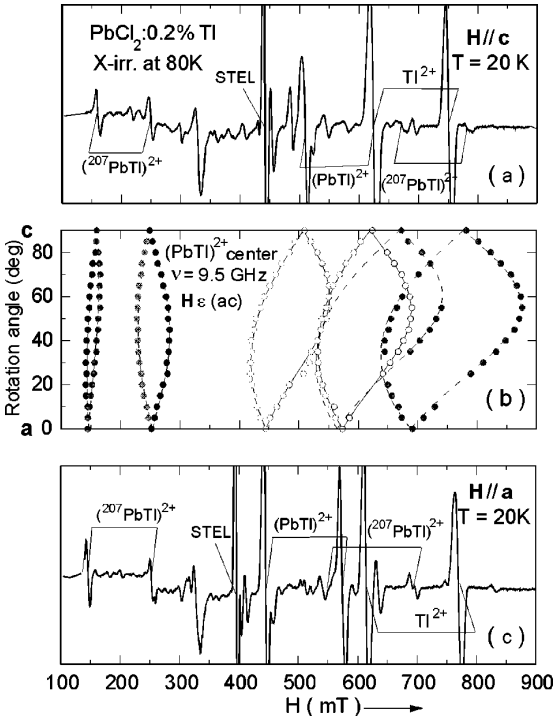

FIG. 1. EPR spectra at $T=20$ K of a $PbCl_2$:Tl crystal, x-ray irradiated at 80 K for 10 min, with the magnetic field along the crystallographic c (a) and a (c) directions. Calculated (solid lines) and experimental (dotted lines) angular variation of the EPR line positions attributed to the $(PbTl)^{2+}$ center are shown for the magnetic field rotated in the ac plane (b).

Besides the lines attributed to the STEL centers[10] and to the Tl^{2+} centers,[17] several additional strongly anisotropic lines with the same production/bleaching properties are observed, suggesting as common origin a new paramagnetic center called $(PbTl)^{2+}$. The corresponding spectrum is composed [Figs. 1(a),1(c)] of an intense central doublet and several weak satellite lines. As shown by a careful analysis of the EPR transitions recorded with the magnetic field rotated in the three main crystal planes, the EPR spectrum is described by the following spin-Hamiltonian:

$$\frac{1}{g_0\mu_B}\mathcal{H}=\frac{1}{g_0}\boldsymbol{H}\cdot\boldsymbol{g}\cdot\boldsymbol{S}+\boldsymbol{S}\cdot\boldsymbol{A}(\mathrm{Tl})\cdot\boldsymbol{I}_1+\boldsymbol{S}\cdot\boldsymbol{A}(\mathrm{Pb})\cdot\boldsymbol{I}_2 \qquad (1)$$

with $S=1/2$. It consists of a Zeeman term and the hyperfine (hf) interaction terms with two nuclei with nuclear spins I_1 and I_2. The hf tensors $\boldsymbol{A}$(Tl) and $\boldsymbol{A}$(Pb) were found to possess different main axes and principal components.

The spin Hamiltonian (1) fully describes the EPR spectrum of a dimer type paramagnetic center containing pairs of Tl and Pb nuclei. Indeed, a spin Hamiltonian containing only the first and second term in Eq. (1) describes the paramagnetic isotopic species containing one of the ^{203}Tl or ^{205}Tl nuclei with $I_1 = 1/2$ (100% total natural abundance) and a ^{even}Pb nucleus with $I_2 = 0$ (78% natural abundance), resulting in the observed central doublet. The full spin Hamiltonian (1) describes the paramagnetic isotopic species containing one of the Tl nuclei and a ^{207}Pb nucleus (22% natural abundance), both with nuclear spin $I_1=I_2 = 1/2$ and different nuclear moments, resulting in the observed satellite lines. Here we have neglected the small difference in the nuclear moments of the two ^{203}Tl and ^{205}Tl nuclei, as the estimated isotopic shift of these nuclei is well inside the experimental linewidths. According to this interpretation the total intensity ratio of the doublet lines to the satellite lines is expected to be roughly 4:1, the ^{even}Pb/^{207}Pb isotopic abundance ratio, in satisfactory agreement with the observed EPR spectra, considering the difficult estimation of the transition probabilities for large hf splittings, especially at low magnetic fields.

The $\boldsymbol{g}$ and $\boldsymbol{A}$(Tl) tensors components and main axes have been determined by a computer diagonalization and fitting procedure involving the positions of the intense EPR doublet lines. The resulting values have been further used in determining the $\boldsymbol{A}$(Pb) tensors components and main axes, by a similar procedure involving the positions of the less intense EPR satellite lines. In the latter case only the parameters describing the $\boldsymbol{A}$(Pb) tensor have been allowed to vary. The resulting spin Hamiltonian parameters are presented in Tables I and II and are compared with the corresponding values of similar dimer type paramagnetic centers. As shown in Fig. 1(b) for one of the main crystal planes, the resulting g_i and A_i values and principal axes fully describe the observed EPR spectra. A similar excellent fitting of the calculated angular dependence and experimental data has been obtained in the other two main crystal planes. Due to the quasiaxial character of the $\boldsymbol{A}$ tensors the estimated accuracy

TABLE I. Principal values and orientation (in degrees) of the $\boldsymbol{g}$ tensors for the dimer $(PbTl)^{2+}$ and Pb_2^{3+} (STEL) centers in $PbCl_2$ and Pb_2^{3+} and Tl_2^{+} impurity dimer centers in alkali chlorides. The orientation of the $\boldsymbol{g}$ tensor main axes is given as the Euler angles for a $R_{zy'z''}(\alpha,\beta,\gamma)$ rotation from the (cba) crystal axes.

Center	T (K)	g_x	g_y	g_z	α	β	γ
$(PbTl)^{2+}$ in $PbCl_2$ [a]	20	1.083	0.994	1.431	24	36	−12
STEL in $PbCl_2$ [b]	10	1.550	1.374	1.719	0	0	10
Pb_2^{3+}(I) in NaCl [c]	15	1.438	1.222	1.625	0	0	0
$Tl_2^{+}\langle 110\rangle$ in KCl [d]	15	1.3094	1.0997	1.7618	0	0	0

[a]Estimated experimental errors in the g components and orientation angles are smaller than ± 0.002 and ± 2, respectively.
[b]From Ref. 10.
[c]From Ref. 7.
[d]From Ref. 18.

TABLE II. Principal values (in mT, absolute values) and orientation (in degrees) of the $\boldsymbol{A}$(Tl) and $\boldsymbol{A}$(Pb) hf tensors of the $(^{\text{even}}\text{PbTl})^{2+}$ and $(^{207}\text{PbTl})^{2+}$ dimer centers, respectively, in comparison with those of the bent Pb_2^{3+} (STEL) center in $PbCl_2$ and the linear Pb_2^{3+} and Tl_2^{+} impurity centers in alkali chlorides. The orientation of the $\boldsymbol{A}$ tensors main axes are given as the Euler angles of a $R_{zy'z''}(\alpha_i, \beta_i, \gamma_i)$ rotation from the (cba) crystal axes.

Center	T (K)	A_x	A_y	A_z	α_i	β_i	γ_i
$(^{\text{even}}\text{PbTl})^{2+}$ in $PbCl_2$ [a]	20	65.9	64.5	85.5	47.8	−4.5	−33.9
$(^{207}\text{PbTl})^{2+}$ in $PbCl_2$ [a]	20	266.6	273.6	223.5	41	32	−44
STEL in $PbCl_2$ [b]	10	−82.8	−85.3	111.7	0	33	0
Pb_2^{3+}(I) in NaCl [c]	15	−122	−117	125	0	0	0
$Tl_2^{+}\langle 110\rangle$ in KCl [d]	15	−259.3	−275.5	190.4	0	0	0

[a]Estimated experimental errors in $A_{x,y,z}$ and β_i are smaller than ± 0.4 and ± 2, respectively. The accuracy of α_i and γ_i is much lower ± 15 due to the quasiaxial character of the $\boldsymbol{A}$(Tl) and $\boldsymbol{A}$(Pb) tensors.
[b]Data for $^{207}\boldsymbol{A}$(Pb) from Ref. 10.
[c]Data for $^{207}\boldsymbol{A}$(Pb) from Ref. 7.
[d]Data for $\boldsymbol{A}$(Tl) from Ref. 18.

in determining the two Euler angles α_i and γ_i defining the orientation of the main axes of the two hf tensors is very low $(\pm 15°)$.

IV. Discussion. The analysis of the EPR spectrum produced in low-temperature x-ray irradiated $PbCl_2$:Tl crystals demonstrates the presence of a paramagnetic dimer center called $(PbTl)^{2+}$, consisting of a Pb^{2+} ion and a neighboring impurity Tl^{+} ion, which have trapped an electron in a bonding molecular orbital.

The identification of the paramagnetic center with a $(PbTl)^{2+}$ molecular center is also supported by the comparable magnitude of the g values and hf parameters with those of the Pb_2^{3+} and Tl_2^{+} impurity dimer centers in alkali chlorides (Tables I and II). It is to be expected that in a similar manner as in the other dimer paramagnetic centers the electron is trapped by the two heavy ions into a bonding σ_g-type molecular ground orbital, which is singly occupied and constructed mainly from atomic $6p$ orbitals with admixture of $6s$ orbitals, centered on the two nuclei. However, due to the strong bending of its molecular bond and the presence of two different nuclei, the analysis of its EPR parameters in terms of a linear molecule, as performed[22] for the other dimer centers does not appear to be adequate.

Additional information concerning the structure and electron properties of the $(PbTl)^{2+}$ center can be derived from the examination of its spin Hamiltonian parameters in comparison with those of other similar dimer type centers, e.g., the STEL center in $PbCl_2$, or the impurity Pb_2^{3+} and Tl_2^{+} centers in alkali chlorides (Tables I and II). Although the g_i and A_i tensors values of the $(PbTl)^{2+}$ center are comparable, a close examination shows significant differences in the orientation of their main axes.

One should mention that for symmetrical molecular centers the principal axes of the $\boldsymbol{g}$ tensor reflect in a good approximation the general orientation of molecule's electron cloud. In particular the g_z component is parallel in a good approximation to the internuclear axis and the principal axes of the $\boldsymbol{A}$ hyperfine tensors reflect the local orientation of the

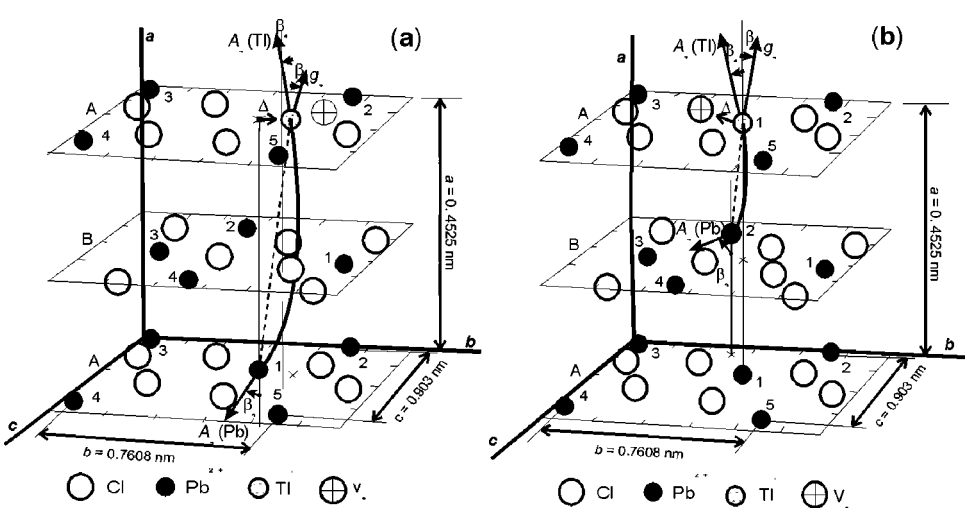

FIG. 2. Expanded structure (along a axis) of the $PbCl_2$ lattice with possible structural models of the $(PbTl)^{2+}$ center and the principal z axes of the $\boldsymbol{g}$ tensor and hf $\boldsymbol{A}$(Tl) and $\boldsymbol{A}$(Pb) tensors as inferred from ESR data. (a) The substitutional model representing a tilted heteronuclear equivalent of the STEL center. (b) The more probable model consisting of an electron trapped at a pair of substitutional Pb^{2+} and Tl^{+} ions in two nearest lattice layers. In both cases a charge compensating anion vacancy next to the Tl^{+} ion is included to account for the observed tilting of the center axis. The lattice cations (numbered) and anions are situated in layers separated by $0.5a$. Distances on the b and c axes are shown by ticks separated by 0.2 nm.

electron cloud at the corresponding nucleus. It means that a different orientation of the A_z and g_z axes reflects a bending of dimer's molecular bond, as previously observed[10] in the case of the STEL center in $PbCl_2$.

We will further discuss the defect model on the basis of the existing crystallographic data.[19,20] The orthorhombic $PbCl_2$ crystal structure (D_{2h}^{16}, $a=0.4525$ nm, $b=0.7608$ nm, and $c=0.0903$ nm) consists of layers of close-packed chlorine and lead ions accommodated in the bc planes (Fig. 2). The lattice ions from neighboring layers (A and B in Figs. 2) of a unit cell are related by inversion symmetry. The only symmetry element (besides the identity) at the Pb^{2+} site is reflection with respect to the bc plane. Moreover, there are two Pb^{2+} sites in each layer related by reflection through ac or ab.

As shown in Fig. 1, of Ref. 11, the self-trapped electron in the STEL center forms a chemical bond between the two nearest-neighbor lattice cations along the a crystal axis. The bending of its bond is reflected in the tilting of the A_z axes by an angle $\beta=33°$ from the a axis, while the direction of the g_z tensor main component is parallel to the a axis.

The examination of $(PbTl)^{2+}$ center's EPR parameters (Tables I and II) strongly suggests that a strong bending of its molecular bond is also present. However, contrary to the STEL center, which has the g_z component along the a crystal direction, parallel to the axis connecting the two Pb nuclei, the Pb-Tl axis of the $(PbTl)^{2+}$ center is tilted away from the a direction by an angle $\beta=36°$, suggesting substantial structural modifications compared to the STEL center.

In the simplest substitutional model one expects the electron produced by radiolysis to be trapped at a pair of nearest-neighbor cations consisting of a Pb^{2+} lattice ion and a substitutional Tl^+ ion separated by $a=0.4525$ nm. The resulting heteronuclear equivalent of the STEL center [Fig. 2(a)] is expected to have its g_z axis parallel to the a axis as well. The presence of a neighboring charge compensating anion vacancy next to the Tl^+ ion in the same lattice layer could explain the observed tilting of the Pb-Tl bond. Such a tilting, together with the expected asymmetry of the electron cloud at the two nucleii, could explain the different tilting angles of the $\boldsymbol{A}$(Tl) and $\boldsymbol{A}$(Pb) hf tensors with respect to the a axis [Fig. 2(a)]. However, it is difficult to accept that a tilting resulting from a possible off-center displacement of the Tl^+ ion could attain values comparable to the measured $\beta=36°$ value, even considering the asymmetry of the electron cloud at the two nuclei. Indeed, in a very rough approximation, based solely on geometrical arguments, one calculates that a $\Delta=0.329$ nm displacement could determine such a tilting. This is a far too large value considering that the largest Pb-Cl distance to the nearest anion in the same layer is only 0.304 nm.

A more likely structure of the $(PbTl)^{2+}$ center results from trapping an electron at a Pb^{2+}-Tl^+ pair consisting of a Pb^{2+} ion and the closest substitutional Tl^+ impurity ion accommodated in the next lattice layer [Fig. 2(b)]. The corresponding upper site A1 occupied by the Tl^+ ion is separated by 0.455 nm from the cation site B2 in the next layer, which is comparable to the $a=0.4525$ nm separation of the Pb-Pb sites involved in the formation of a STEL center (the distance to the other neighbor cation sites from the same layer B are larger: 0.488 nm to site B4 and 0.505 nm to sites B1 and B3). Moreover, in the pure $PbCl_2$ lattice the connecting axis of these two sites makes an angle of $\approx 60°$ with the a axis. The difference with the $\beta=36°$ tilting of the g_z main axis from the a direction can be explained, as shown in Fig. 3(b), by an off-center displacement of the Tl^+ ion due to the possible presence of a neighboring charge compensating anion vacancy combined with a certain asymmetry of the electron cloud at the two nuclei. The tilting of the hf tensors $\boldsymbol{A}$(Tl) and $\boldsymbol{A}$(Pb) from the a axis with $\beta_1=-4.5°$ and $\beta_2=32°$, respectively, can be more easily explained in this model as resulting from a combined tilting and bending of the $(PbTl)^{2+}$ center and a certain degree of asymmetry of the electron cloud at the two nuclei.

Another possible structure of the $(PbTl)^{2+}$ center, which could be considered, would involve the presence of interstitial thallium ions (atoms). However, this hypothesis can be ruled out considering the results of ionic conductivity measurements[21] on $PbCl_2$ crystals doped with TlCl, which have shown that thallium enters the crystal lattice as substitutional Tl^+ at cation sites, with a proportional increase in the concentration of charge compensating anion vacancies. In fact, it may be that the presence of the charge compensating vacancy next to the Tl^+ ion favors the electron trapping at a Pb^{2+}-Tl^+ pair situated in nearest layers as illustrated in Fig. 2(b).

We have neglected here the unlikely possibility of an electron being trapped at two lattice cations from the same layer, as this would result in the g_z component being oriented in the bc plane, which was not observed experimentally.

Finally, one should mention that the formation of such a $(PbTl)^{2+}$ heteronuclear trapped-electron dimer center suggests the possibility of employing specific cation impurities as activating centers in the photolytic formation of colloidal lead in $PbCl_2$. Moreover, such impurities may play an important role as localization sites in the formation of trapped excitons, with influence on their recombination properties.

This work was performed under the auspices of a bilateral Flemish-Romanian cooperative scientific research project to which the authors are greatly indebted. One of the authors (E.G.) gives thanks to the Fund for Scientific Research Flanders (FWO) for financial support.

*Permanent address: Institute of Atomic Physics (NIMP), P.O. Box MG 7 Magurele, Bucuresti, 76900 Romania.

[1] J. F. Verwey, J. Phys. Chem. Solids **31**, 163 (1970), and references cited therein.

[2] W. C. De Gruitjter and J. Kerssen, J. Solid State Chem. **5**, 467 (1972); **10**, 837 (1972).

[3] A. V. Patankar and E. E. Schneider, J. Phys. Chem. Solids **27**, 575 (1966); Proc. Brit. Ceram. Soc. **9**, 97 (1967).

[4] J. Arendts and J. F. Verwey, Phys. Status Solidi **23**, 137 (1967).

[5] E. Goovaerts, J. Andriessen, S. V. Nistor, and D. Schoemaker, Phys. Rev. B **24**, 29 (1981).

[6] E. Goovaerts, S. V. Nistor, and D. Schoemaker, Phys. Rev. B **28**, 3712 (1983).

[7] I. Heynderickx, E. Goovaerts, S. V. Nistor, and D. Schoemaker, Phys. Status Solidi B **136**, 69 (1986).
[8] I. Heynderickx, E. Goovaerts, and D. Schoemaker, Phys. Rev. B **36**, 1843 (1987).
[9] E. Goovaerts, S. V. Nistor, and D. Schoemaker, J. Phys.: Condens. Matter **4**, 9259 (1992).
[10] S. V. Nistor, E. Goovaerts, and D. Schoemaker, Phys. Rev. B **48**, 9575 (1993); **52**, 12 (1995).
[11] S. V. Nistor, E. Goovaerts, and D. Schoemaker, Radiat. Eff. Defects Solids **136**, 157 (1995).
[12] D. Schoemaker, Phys. Rev. B **7**, 786 (1973).
[13] W. C. De Gruijter, J. Solid State Chem. **6**, 151 (1973).
[14] G. Liidja and V. L. Plekhanov, J. Lumin **6**, 71 (1973), and earlier references cited therein.
[15] M. Kitaura and H. Nakagawa, J. Electron Spectrosc. Relat. Phenom. **79**, 171 (1996).
[16] S. V. Nistor, M. Stefan, and I. Ursu, Solid State Commun. **85**, 983 (1993).
[17] S. V. Nistor, E. Goovaerts, and D. Schoemaker, Solid State Commun. **96**, 491 (1995).
[18] B. R. Yang, E. Goovaerts, and D. Schoemaker, Phys. Rev. B **27**, 1507 (1983).
[19] A. Ranfagni, D. Mugnai, M. Bacci, G. Viliani, and M. P. Fontana, Adv. Phys. **32**, 823 (1983).
[20] R. W. G. Wyckoff, *Crystal Structures* (Wiley, New York, 1963), Vol. 1.
[21] K. J. De Vries and J. H. Santen, Physica (Amsterdam) **29**, 482 (1963).
[22] S. V. Nistor and D. Schoemaker, Phys. Status Solidi B **190**, 339 (1995).